QdG
ISSN 1590-2595
Anno 2010_Numero 80

Site effects at the Campi Flegrei, preliminary results

Quaderni di
Geofisica

80

Istituto Nazionale di
Geofisica e Vulcanologia

Quaderni di Geofisica

Segreteria di Redazione
Francesca Di Stefano - coordinatore
Tel. +39 06 51860068
Fax +39 06 36915617
Rossella Celi
Tel. +39 06 51860055
Fax +39 06 36915617

redazionecen@ingv.it

ISSN 1590-2595
Anno 2010_Numero 80

Site effects at the Campi Flegrei, preliminary results

Effetti di sito ai Campi Flegrei, risultati preliminari

Anna Tramelli, Danilo Galluzzo, Mauro A. Di Vito

INGV (Istituto Nazionale di Geofisica e Vulcanologia, Sezione di Napoli - Osservatorio Vesuviano)

In copertina Campi Flegrei (particolare)

Site effects at the Campi Flegrei, preliminary results

The Campi Flegrei caldera is a complex structure with a high population density, located west of the city of Naples. In addition of being an active volcano it is characterized by a high seismic hazard due to both Appennines regional earthquakes and to local earthquakes occurring during the bradyseismic crises. These unrest phenomena are characterized by slow ground vertical movements, particularly active in the central part of the caldera, and by a high number of low-magnitude earthquakes.
In this context, the determination of the site transfer functions of the area has a strong relevance for the Civil Defense aimed to determine the hazard of the area. We have calculated the site transfer function with different techniques (H/V and Generalized Inversion technique) and have collected data on the local geology with the aim of correlating the site transfer functions with lithology and topography. This analysis has been performed on three areas: the Astroni crater, the Camaldoli hill and the Agnano plain. A future development will be to extend this analysis to the whole Campi Flegrei area.

La caldera dei Campi Flegrei è una struttura complessa con un elevata densità di popolazione che si trova ad ovest della città di Napoli. Oltre ad essere un vulcano attivo quest'area risente dei terremoti degli Appennini e dei terremoti dovuti a fenomeni bradisismici. Il fenomeno del bradisismo consiste in un lento movimento verticale, particolarmente attivo nella parte centrale della caldera e spesso accompagnato da terremoti di bassa magnitudo.
In questo contesto, la determinazione della funzione di trasferimento di sito dell'area è di fondamentale importanza per il Dipartimento della Protezione Civile al fine di definire il rischio sismico dell'area. In questo lavoro è stata calcolata la funzione di trasferimento di sito utilizzando tecniche diverse: H/V e metodo delle inverse generalizzate. Questi risultati sono stati integrati con le informazioni sulla geologia locale allo scopo di correlare la funzione di amplificazione di sito con la litologia e la morfologia locali. Quest'analisi è stata applicata a tre aree particolari: il cratere degli Astroni, la collina dei Camaldoli e la piana di Agnano. In futuro l'analisi verrà estesa a tutta l'area dei Campi Flegrei.

Introduction

A critical factor for seismic hazard estimation is a detailed evaluation of the site response. Seismic shaking is highly influenced by the local physical and mechanical properties of the rocks underlying a site. Shallow or thick sedimentary deposits can significantly amplify the earthquake ground motion. Seismologists and engineers have conducted numerous studies to quantify how the seismic energy is modified and how structures that overlie vulnerable soils will behave during strong ground shaking [Wills et al., 2000].
Different methods can be applied to estimate the site response from seismic records. The most frequently used is the spectral ratio method. This approach needs the identification of a reference site, usually characterized by outcropping lithoid rocks, and consists in computing the ratio between the spectrum at a site of interest with respect to the reference site spectrum [Borcherdt and Gibbs, 1976]. Both S waves [Field et al., 1995] and coda waves [Phillips and Aki, 1986] can be used for this application. One of the advantages of using the coda waves is that their propagation depends only on average regional properties of the medium and is independent on the source and recording site locations. Other methods, called inversion method [Andrews, 1986; Boatwright et al., 1991], cast the problem into a formalized inversion that is based on the assumption that the observed earthquake spectrum can be decomposed into a source, path and site terms. This method does not make any assumption on the source spectra and allows to determine the site transfer function with respect to a reference site or to the average response of all the other sites [Phillips and Aki, 1986]. These methods depend on the used reference spectrum. An alternative technique that does not need a reference site is the so called H/V method, which uses the ratio between the

horizontal and vertical spectra of the S-wave (or the coda wave) window for each site [Lermo and Chàvez-Garcìa, 1993]. The assumption of this method is that the local site conditions are relatively transparent to the motion that appears on the vertical component, whether they affect the horizontal components.

In this paper we apply the inversion and H/V method to the data collected by three networks installed in the area of Campi Flegrei in different times. The applied method depends on the type of data, earthquakes or noise recordings. Our results are then compared with the results obtained by Del Pezzo et al. [1993] in the Campi Flegrei area during the 1982-84 bradyseismic crises. The results are related to the local geological properties with the aim of extending the punctual site information (the site transfer function is calculated for the point where the station lies) to an area characterized by the same geological properties.

1. The Campi Flegrei caldera structure and evolution

The Campi Flegrei caldera is one of the three active volcanoes of the Neapolitan area [Santacroce et al., 2003]. The geology of this caldera has attracted the interest of many Earth scientists. Orsi et al. [1996] have proposed the most recent comprehensive reconstruction of the volcanic and deformation history of the Campi Flegrei area, as well as detailed references of previous works. The Campi Flegrei caldera results from two main nested collapses related to the Campanian Ignimbrite (39 ka) and Neapolitan Yellow Tuff (NYT, 15 ka) eruptions, respectively. Portions of the margins of both calderas results by reactivation of NE-SW and NW-SE trending regional faults. After each collapse, volcanism has been confined within the collapsed area. In the past 15 ka, volcanism has occurred within the NYT caldera and has been strictly related to the deformation of this structure. It has been concentrated in three epochs of activity, dated 15-9.5, 8.6-8.2 and 4.8-3.8 ka, with the last eruption, which generated the Mt Nuovo tuff cone in 1538 AD, after a long quiescence [Di Vito et al., 1999]. The three epochs of activity were separated by periods of quiescence, marked in the field by two paleosols. During each epoch eruptions occurred one after the other with average time intervals of few tens of years. During the past 10 ka, the NYT caldera floor was affected by resurgence which generated ground uplift and subsidence with consequent emersion and submersion of the caldera floor [Cinque et al.; 1984; Orsi et al., 1996; Di Vito et al., 1999]. During the quiescence between the II and III epoch, resurgence acquired its apex and the caldera floor emerged before the beginning of the III epoch. Historical ground deformation within the NYT caldera has been documented at the Serapeo, a Roman market-place in Pozzuoli, for at least the past 2 ka [Parascandola, 1947]. Two major bradyseismic episodes have generated 170 cm of ground uplift in 1969-72 and 180 cm in 1982-84 followed by minor uplift episodes in 1989 (7 cm), 1994 (1 cm), 2000 (4 cm), 2004-06 (6 cm) [Barberi et al., 1984; Orsi et al., 1999 and references therein; Del Gaudio et al. 2009]. All these uplift episodes were accompanied by low magnitude seismicity [Orsi et al, 1999].

The volcanic and deformation history of the Campi Flegrei caldera, including its magmatic feeding system, as well as its present state, demonstrate that the system is active and can erupt again.

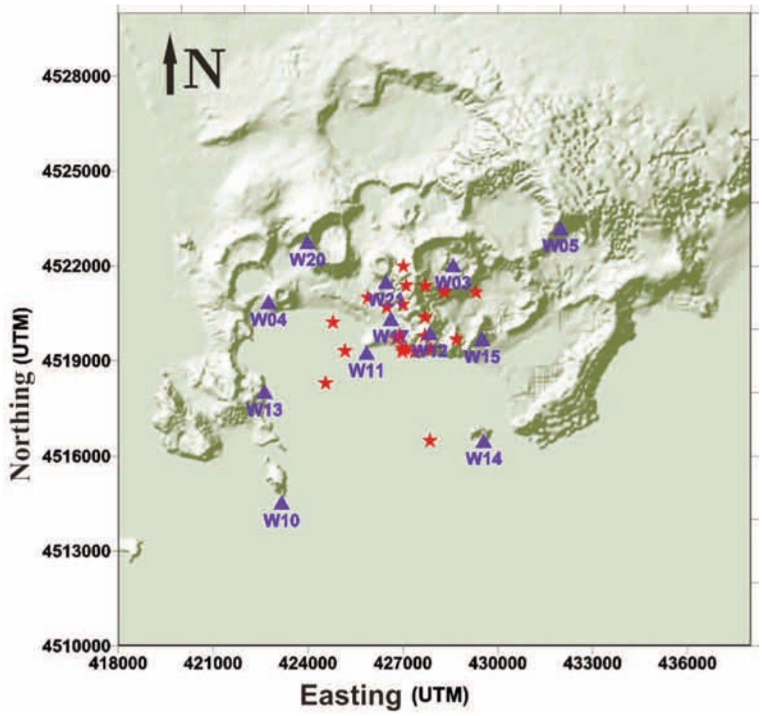

Figure 1 DTM of the Campi Flegrei area. Purple triangles: Wisconsin Network stations; red stars: the earthquakes recorded during the 1982-84 bradyseismic crises used for the analysis. UTM coordinates are in meters.
Figura 1 DTM dell'area dei Campi Flegrei. Triangoli viola: stazioni appartenenti al Wisconsin Network; stelline rosse: terremoti registrati durante la crisi bradisismica del 1982-84 usati in questa analisi. Le coordinate UTM sono in metri.

2. Data set

The seismic data used for the analysis of the site effects in the area of Campi Flegrei can be divided into three sets:

1) data recorded by the seismic network of the University of Wisconsin (WN);
2) data recorded by the seismic mobile network of the INGV, Osservatorio Vesuviano (MSN);
3) data collected during the active seismic experiment called SERAPIS (SE).

2.1 Wisconsin Network

The first set of data was recorded during the 1982-1984 bradyseismic crisis that was characterized by a maximum uplift of more than 1.7 m [Aster et al., 1989] recorded in the area of the 'Accademia' of Pozzuoli. During this crisis thousands of shallow (depth ≤ 3 km), low-magnitude (up to Md=4.0) earthquakes were recorded. Seismic activity was more intense during March and April 1984, with a large swarm on April 1st. The seismic events were recorded by a network deployed by the University of Wisconsin, composed by short-period, three-component, high-dynamic range (106 dB) digital stations (blue triangles in Fig. 1) and locally recorded on tapes in PCM format [Del Pezzo et al., 1984].
Data were recorded with different sampling rates, sometimes changed during the survey (table I). To overcome this problem we later resampled all records at 100 sps.
After a visual inspection of the recordings we decided to discard station W11 because of the high instrumental noise. For the station W15 we noticed that since 29/02/1984 at 10:27 the EW and Vertical components were exchanged, consequently we exchanged them back.
The response curve is almost identical for all stations. To get the amplitude in m/s signals are divided for the instrument sensitivity 36 V/inch/s and multiplied by the conversion factor 0.0056 m/inch. The data sheet of 1980 reporting the transfer function of the WN sensors is shown in Fig. 2.
To check this procedure, we visually compared the amplitu-

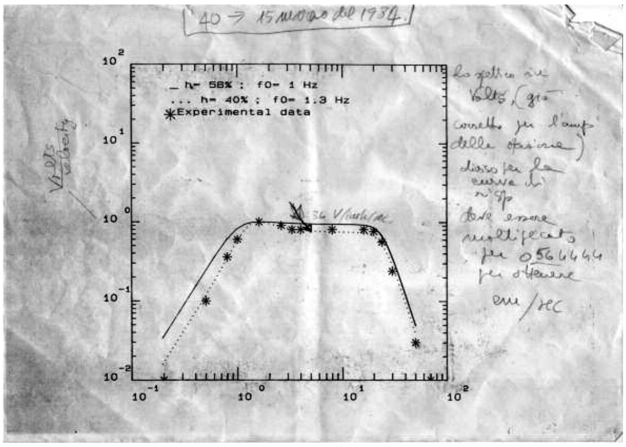

Figure 2 Data sheet of the 1984 reporting the transfer function of the Wisconsin Network sensors.
Figura 2 Appunti del 1984 che riportano la funzione di trasferimento dei sensori appartenenti al Wisconsin Network.

Name	Site	Latitude N	Longitude E	Elevation (m a.s.l.)	Sampling (Hz)
W03	Astroni	40.8462	14.1528	35	100
W04	Mt. Nuovo	40.8352	14.0838	70	100
W05	Camaldoli	40.8570	14.1930	457	100
W10	Capo Miseno	40.7782	14.0895	50	100
W11	Darsena	40.8210	14.1208	82	200
W12	Solfatara	40.8267	14.1443	180	100
W13	Castello Baia	40.8097	14.0827	20	200
W14	Nisida	40.7963	14.1650	40	100
W15	Mt. Spina	40.8252	14.1640	150	100
W17	Starza Est	40.8307	14.1297	84	100
W20	Mt. S. Angelo	40.8523	14.0982	306	100-200
W21	Fondi Cigliano	40.8412	14.1278	175	100

Table I Locations and sampling rates of the stations belonging to the Wisconsin Network.
Tabella I Localizzazioni e frequenze di campionamento delle stazioni appartenenti al Wisconsin Network.

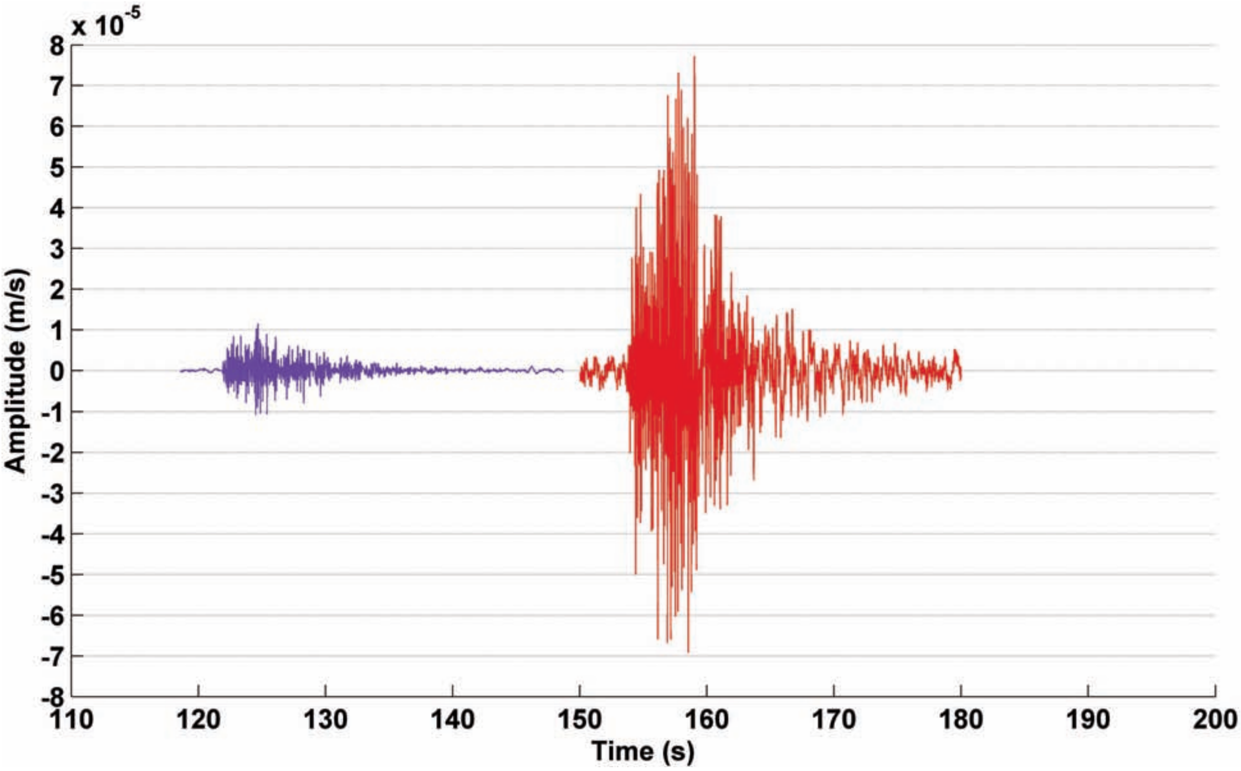

Figure 3 Seismograms for the two seismic events of table II. The seismogram of the earthquake 126 recorded by station W04 is in purple, the seismogram of the earthquake 6019 recorded by station OMN2 is in red.
Figura 3 Sismogrammi relativi ai due terremoti riportati in tabella II. Viola: terremoto 126 registrato dalla stazione W04; rosso: terremoto 6019 registrato dalla stazione OMN2.

de of earthquakes with similar magnitude and hypocentral-station distance recorded during the two different periods (1982-84 and 2006-08). As an example we show two earthquakes with magnitude M=1.3 and 1.4 (see table II), the first one recorded during the 1982-84 bradyseismic event and the second recorded in 2006. We selected the W04 (WN) and OMN2 (MN) stations located close to each other, on the Mt. Spina hill, at a distance of 592 m (see Figs. 1 and 4). The recordings of the two earthquakes are shown in Fig. 3. The maximum amplitude ratio between the two signals is compatible taking into account the magnitude difference and the errors in the magnitude values.
We used only events recorded by more than 6 stations. The final data set includes 22 events, shown in Fig. 1, recorded in SAC format and corrected for the instrument transfer function.
The coordinates of the used stations are reported in table I.

2.2 Mobile Seismic Network

The seismic events occurred in 2006 and 2008 were recorded by the Mobile Seismic Network (MSN) stations. MSN is still working in the Campi Flegrei area in continuous acquisition modality and is composed by 7 high-dynamic (20 bit) digital stations, 6 equipped with broadband sensors (LE3D 20s and GURALP CMG40T 60s) and 1 with short-period sensor (LE3Dlite 1Hz) (table III). Timing signal was synchronized with external GPS, sampling rates are set to 100 or 125 sps. The stations are located in the central part of Campi Flegrei

Earthquake	M	Date	Latitude N (m)	Longitude E (m)	Depth (m b.s.l.)	Rec. Station
126	1.3	26/01/1984	4518309	424557	3650	W04
6019	1.4	24/12/2006	4521625	427921	1190	OMN2

Table II Events used for the comparison between the Wisconsin Network and the Mobile Seismic Network. Geographic coordinates are UTM 33.
Tabella II Eventi utilizzati per il confronto tra il Wisconsin Network e Mobile Seismic Network. Le coordinate sono UTM33.

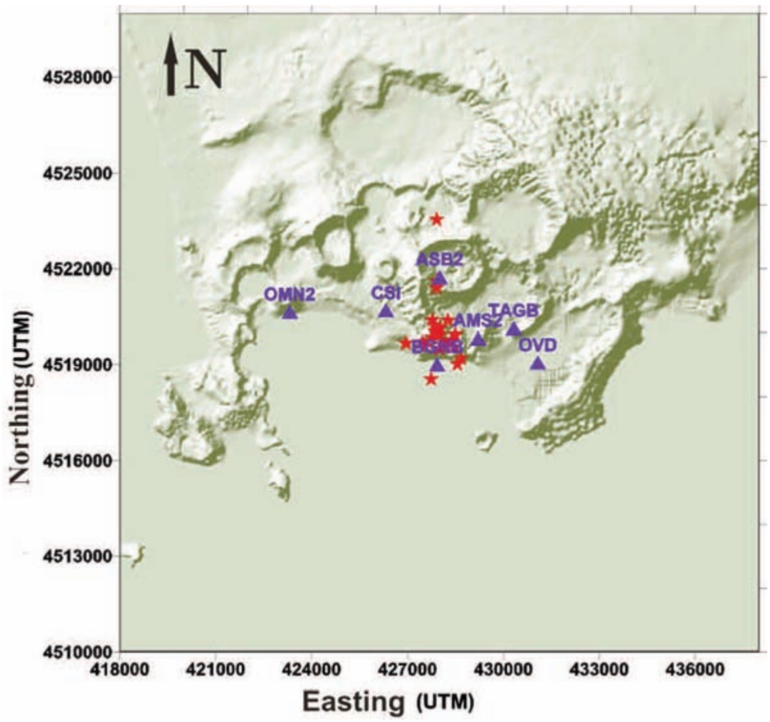

Figure 4 DTM of the Campi Flegrei area with the stations belonging to the Mobile Seismic Network (purple triangles) and the earthquakes (red stars) used for the analysis. The UTM coordinates are in meters.
Figura 4 DTM dell'area dei Campi Flegrei. Triangoli viola: stazioni appartenenti al Mobile Seismic Network; stelline rosse: terremoti utilizzati nell'analisi. Le coordinate UTM sono in metri.

as shown in Fig. 4. The transfer functions of the MSN sensors are reported in Fig. 5.
The data set used for the evaluation of the site response is composed by recordings of local earthquakes (red stars in Fig. 4) and seismic noise. The amplitude of the waveforms (SAC format) is recorded in microvolt and, to obtain a uniform data set in agreement with the WN one, we divided for the instrument transduction of the sensors (reported in table III) to obtain the amplitude in m/s. As shown in Fig. 5 the sensor transfer functions are flat in the frequency window 1-20 Hz used for the analysis.
The final data set includes 27 events.

2.3 SERAPIS Network

This temporary network was deployed in the area of Campi Flegrei during the SERAPIS experiment (SEismic Reflection/Refraction Acquisition Project for Imaging complex volcanic Structures), carried out in September 2001. The source and receiver arrays covered an area of more than 50 x 50 km², including the bays of Napoli and Pozzuoli [Judenherc and Zollo, 2005]. For two weeks the ship Le Nadir produced source-shots with an air gun inside the bay of Pozzuoli following a grid of

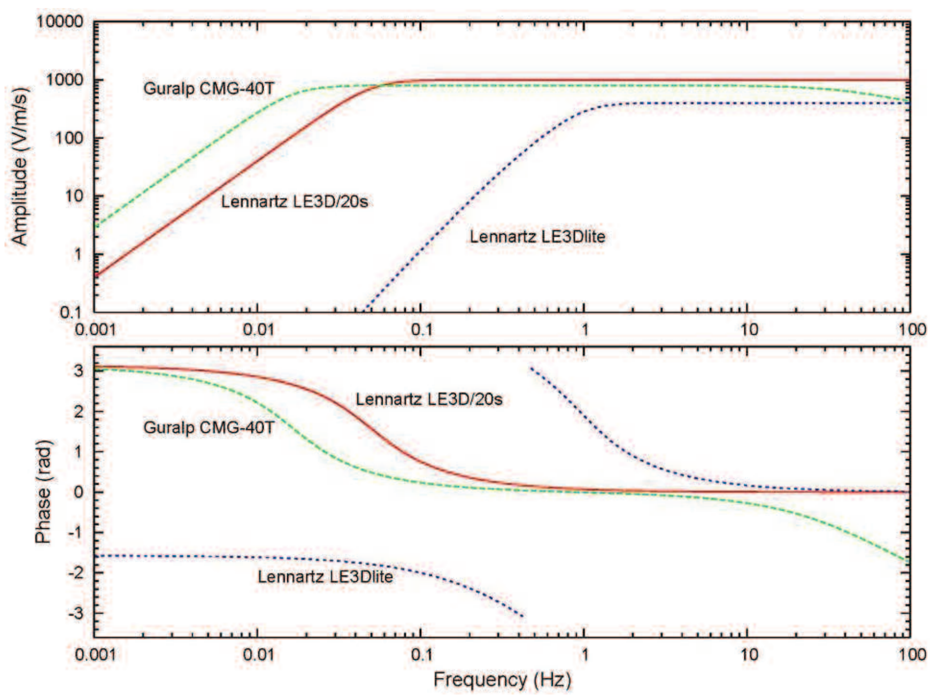

Figure 5 Amplitude (top) and phase (bottom) of the transfer functions for the three sensors used in the Mobile Seismic Network.
Figura 5 Ampiezza (sopra) e fase (sotto) della funzione di trasferimento per i tre diversi sensori utilizzati dal Mobile Seismic Network.

Name	Data Logger	Sensor	Transduction (V*s/m)
AMS2	Lennarz MARSlite	LE-3D/20s	1000
ASB2	Lennarz MARSlite	LE-3D/20s	1000
BGNG	Lennarz M24	Guralp CMG40T	800
CSI	Lennarz PCM5800	LE-3Dlita 1 Hz	400
OMN2	Lennarz MARSlite	LE-3D/20s	1000
OVD	Lennarz M24	LE-3D/20s	1000
TAGG	Taurus	Guralp CMG40T	800

Table III Sensors, data loggers and gains of the stations belonging to the Mobile Seismic Network.
Tabella III Sensori, *data logger* e *Gain* delle stazioni appartenenti al Mobile Seismic Network.

N-S and E-W lines [Gasparini, 1998]. The on-land acquisition array was designed to provide a very high density coverage and consisted of 18 vertical and 66 three-component seismometers continuously recording during the experiment. We selected 34 three-component stations and analyzed the seismic noise recorded during the experiment; the stations used for the site effects analysis are shown in Fig. 6 and their coordinate are reported in table V.
The data set selected for this analysis is composed by 100 minutes of seismic noise for each station (100 files of 60 s each). The original format of the data was Segy, then converted into ASCII.

2.4 Earthquakes location

The seismic events used for the site transfer function analysis recorded by both the WN and MSN were picked manually for P and S first arrivals. Unfortunately, the magnitude of the events recorded by the MN between 2005 and 2007 was low and the signal-to-noise ratio was often unfavorable to pick the S wave onset. In these cases we forced the S wave first onset at 1.7 times the P wave travel time. We choose earthquakes recorded by at least 6 stations for the WN, as mentioned before, and 3 stations for the MSN. We used the NonLinLoc program [Lomax et al., 2000] that determines the location of the hypocenters within a 3D Grid using a systematic grid-search. For the earthquakes recorded only by 3 MSN stations we used also the picking of the 1D stations located in the Campi Flegrei area to correctly locate the hypocenters. The velocity model used for the location is the one proposed by Judenherc and Zollo [2005]. The location of the earthquakes is reported in Fig. 1 for the WN and in Fig. 4 for the MSN (red stars).

3. Method of analysis for site effects estimation

We estimated the site amplification with different techniques depending on the available data set.
As for the data set collected by the WN and MSN, composed of earthquake records, we analyzed the S and coda waves while for the data recorded by the SN we analyzed the seismic noise.
We calculated the site transfer function using the generalized inversion (GI) method [Hartzell, 1992; Bonilla et al., 1997; Parolai et al., 2001; Drouet et al., 2005], the coda inversion (CI) technique [Tsujiura, 1978; Bonilla et al., 1997] and the horizontal to vertical spectral ratio (H/V) applied on the S waves and/or on the coda waves [Langston, 1979]. For the S-wave analysis we considered a time window of 3 s starting 0.1 s before the S-wave arrival; for the coda waves we considered a window of 3 s starting at 8 s of lapse time. Only the H/V technique was applied to the seismic noise [Nakamura, 1989]. The lack of bedrock sites leads us to consider the average spectrum between all of the investigated sites as the

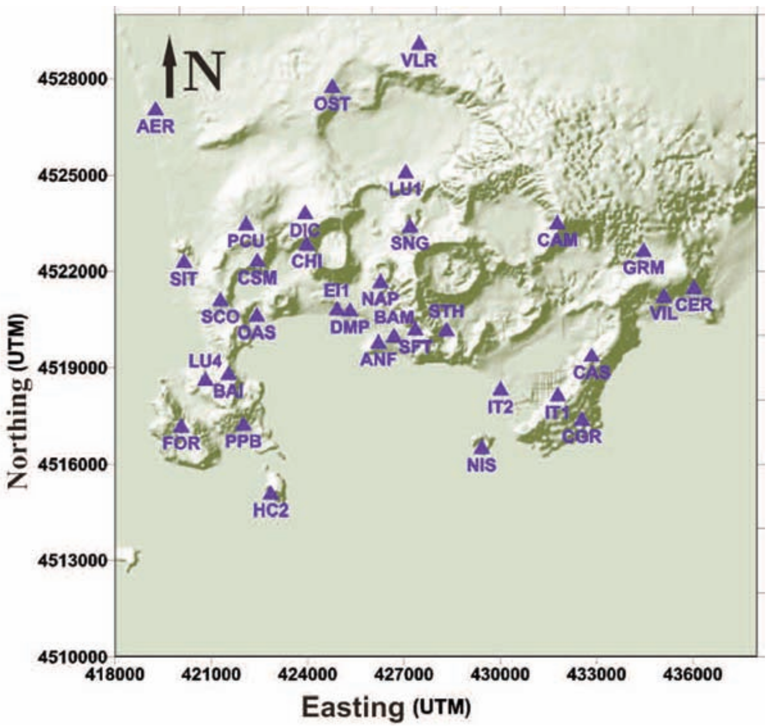

Figure 6 DTM of the Campi Flegrei area with the stations belonging to the SERAPIS Network (purple triangles). The UTM coordinates are in meters.
Figura 6 DTM dell'area dei Campi Flegrei con le stazioni appartenenti al SERAPIS Network (triangoli viola). Le coordinate UTM sono in metri.

Name	Site	Latitude N	Longitude E	Elevation (m a.s.l.)	Sampling (Hz)
AMS2	Mt. Spina	40.8264	14.1604	35	125
ASB2	Astroni	40.8435	14.1459	12	125
BGNG	Bagnoli	40.8189	14.1454	4	125
CSI	Pozzuoli	40.8340	14.1262	89	125
OMN2	Mt. Nuovo	40.8333	14.0904	40	125
OVD	Osservatorio	40.8197	14.1827	14	100
TAGG	Terme Agnano	40.8293	14.1736	4	100

Table IV Locations and sampling rate of the stations belonging to the Mobile Seismic Network.
Tabella IV Localizzazione e frequenza di campionamento delle stazioni del Mobile Seismic Network.

reference spectrum. This assumption was made for the GI method applied on the S-waves and for the CI method applied on the coda waves. An extensive description of the used method can be found in Galluzzo et al. [2009].
We corrected the amplitude spectra for the geometrical spreading and for the quality factor Q of the S-waves for the GI method and of the coda waves for the CI method. The propagation effects of S and coda waves can be respectively written as:

$$P_S(\omega) = \frac{\exp(-\frac{\omega D}{2Q_S v})}{D} \qquad P_C(\omega, t) = \frac{\exp(-\frac{\omega t}{2Q_C})}{D}$$

where ω is the angular frequency, D is the hypocenter-station distance, t is the lapse time and v is the S wave velocity. Q_S is the S-wave quality factor and Q_C is the coda-wave quality factor. For the analysis we used the quality factor estimated by Petrosino et al. [2008].
The data set available for the application of the GI method was limited, due to the difficulty of identifying the S onset. On the contrary, coda waves are particularly suitable to compute the site transfer function since they are not affected by radiation pattern effects and, in a limited area, have the same propagation effects of the direct S waves [Tsujiura, 1978; Lachet et al., 1996; Bonilla et al., 1997]. For this reason we used the CI method to confirm the results obtained with the GI technique.
The aim was thus to compare the results of the site-transfer function for each site obtained with these different methods. The comparison was made in terms of peak frequencies and relative amplitudes of the evaluated site-transfer functions. To evaluate the differences between the different methods, the uncertainties of each method were also calculated.

4. Geological characteristics of selected areas with particular site amplification

The Campi Flegrei area has been investigated for long time due to the high volcanological, seismological and geothermal interest [Rosi and Sbrana, 1987; Orsi et al., 1996]. Thus we benefit of a wide geological information to properly characterize the analyzed sites.
The structural features of Campi Flegrei result mostly from alternating constructive and destructive volcanic events. Effusive eruptions produced small lava domes, medium- and low-magnitude explosive eruptions generated tuff cones, tuff rings and pumice and scoria cones, high-magnitude explosive events generated widespread pyroclastic fallout and pyroclastic current deposits [Di Vito et al., 1999; Orsi et al., 2004]. Furthermore, the high-magnitude events determined the occurrence of tectonic collapses (i.e., the Campanian Ignimbrite and Neapolitan Yellow Tuff calderas and the Agnano volcano-tectonic collapse) [Orsi et al., 1996; de Vita et al., 1999]. After the collapse events the depressed part of Campi Flegrei was invaded by the sea, with related erosional and depositional processes. Consequently, the Campi Flegrei area is mostly composed of volcanic rocks and subordinately of palustrine and marine clastic sediments [Orsi et al., 1996]. The geological features of the area are described in Di Vito et al. [1999] who investigated the area through geomorphological and geological surveys. The flat

Name	Site	Latitude N	Longitude E	Elevation (m a.s.l.)	Sampling (Hz)
AER	Varcaturo	40.8909	14.0416	3	125
ANF	Anfiteatro Flavio	40.8261	14.1249	30	125
BAI	Baia	40.8168	14.0695	60	125
BAM	Starza Est	40.8279	14.1306	81	125
CAM	Camaldoli	40.8601	14.1906	400	125
CAS	Via Campegna	40.823	14.2037	60	125
CER	Certosa S. Martino	40.8423	14.2412	206	125
CGR	Posillipo	40.805	14.2002	113	125
CHI	S. Angelo	40.8534	14.098	206	125
CSM	Monterusso	40.8487	14.0798	70	125
DIC	Masseria Castaldi	40.8622	14.0972	176	125
DMP	Gauro	40.835	14.1142	46	100
EI1	Olivetti	40.8353	14.1094	40	125
FOR	Mt. Procida	40.802	14.0524	100	125
GRM	Vomero	40.8525	14.2225	175	125
HC2	Capo Miseno	40.7835	14.0857	109	125
IT1	Italsider	40.8118	14.1912	26	125
IT2	Italsider	40.8132	14.1701	4	125
LU1	Quarto Sud	40.874	14.1342	46	125
LU4	Torre Cappella	40.8151	14.061	20	125
NAP	Fondi Cigliano	40.8431	14.1253	180	125
NIS	Nisida	40.7968	14.1633	3	100
OAS	Lucrino	40.8333	14.0798	25	125
OST	Monteleone	40.8977	14.1068	93	125
PCU	Monteruscello	40.859	14.0755	95	125
PPB	Bellavista	40.8027	14.0753	62	125
SCO	Scalandrone	40.8376	14.0663	120	125
SFT	Solfatara	40.8298	14.1385	100	100
SIT	Cuma	40.8481	14.0526	90	125
SNG	Discarica Fossa Lupara	40.8588	14.136	63	125
STH	Tennis Hotel	40.8297	14.15	150	100
VIL	Villa Floridiana	40.8398	14.2301	100	125
VLR	Giugliano	40.9101	14.1387	160	125

Table V Locations and sampling rate of the stations belonging to the SERAPIS Network.
Tabella V Localizzazioni e frequenza di campionamento delle stazioni del SERAPIS Network.

areas were investigated by using boreholes drilled in the areas of Fuorigrotta, Agnano, Toiano, Pianura, Soccavo and La Starza (see Fig. 7). In the active part of the Campi Flegrei caldera they recognized at least 70 pyroclastic units, composed of both loose pyroclastic rocks and welded or zeolitized, cohesive, and few lava units forming lava domes. In the flat areas thick marine and beach deposits composed of coarse to fine sand are intercalated with volcanic deposits. In Agnano and along the Fuorigrotta coast soft silt and peat marsh deposits were cored (Fig. 7).

On the basis of sedimentological and lithological characteristics, the different types of deposits have been grouped as follows:

Type A: loose pyroclastic deposit;
Type B: welded or lithified, cohesive tuffs;
Type C: lavas;
Type D: marine and palustrine deposits.

We collected geological data of selected sites of Campi Flegrei in which the seismic stations are located to associate the site transfer function information to geological characteristics. Thus the site transfer function information have been extended to the area surrounding the seismic stations with the same geological characteristics.

Some of the site transfer functions show high peaks in the frequency band 1-10 Hz. These sites are the most interesting for seismic hazard estimation; we decided to make an intensive analysis on the geological characteristics of the station sites: W03, ASB, W05 and TAG.

4.1 The Astroni crater

Station W03, belonging to the WN, and station ASB2 belonging to the MSN were located inside the Astroni crater (bottom left panel of Fig. 8). This crater is 2 km wide, and was formed during the recent Campi Flegrei activity [Di Vito et al., 1999]. The Astroni crater floor is filled by loose, partially reworked pyroclastic sediments, overlying small lava domes (type C deposit) and a tuff cone (type B deposit) formed during the final Astroni activity.

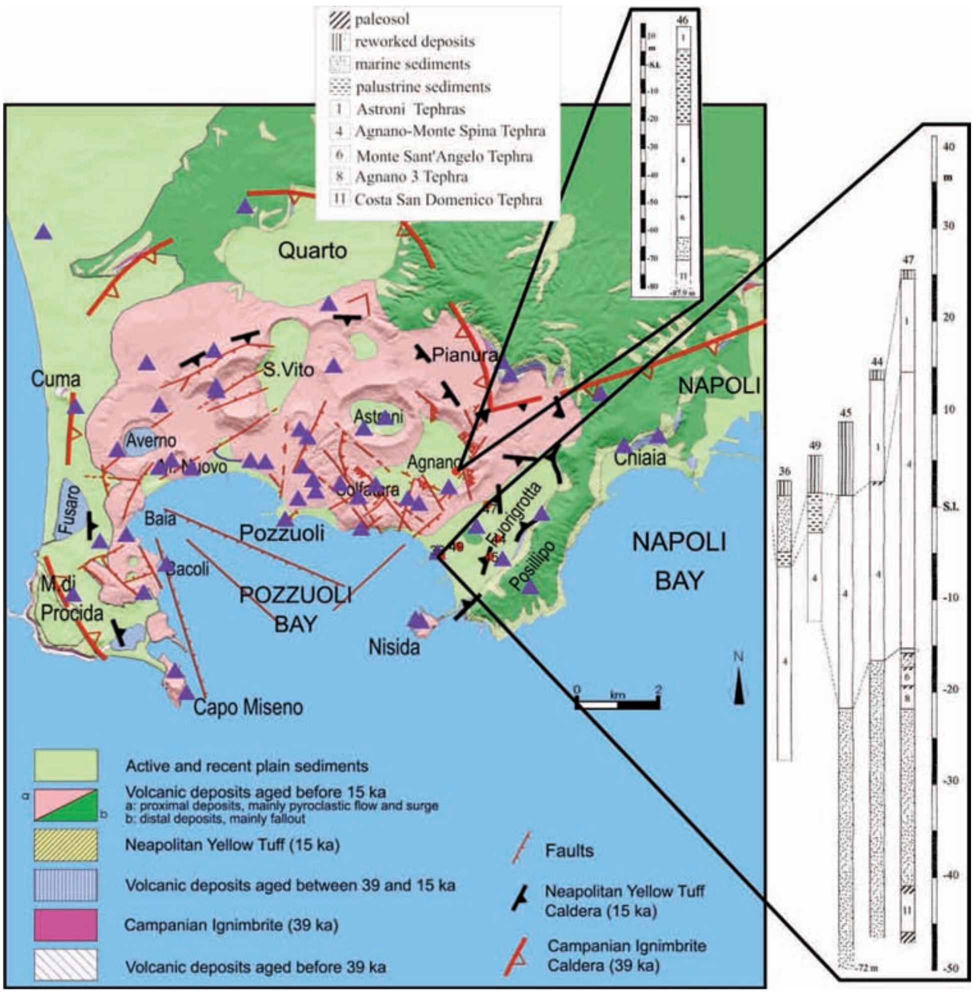

Figure 7 Geological sketch map of the Campi Flegrei area published by Orsi et al. [1996]. The purple triangles represent the seismic stations of the Wisconsin Network, Mobile Seismic Network and SERAPIS Network used for the site analysis.

Figura 7 Mappa geologica dei Campi Flegrei pubblicata da Orsi et al. [1996]. I triangoli viola rappresentano le stazioni sismiche di Wisconsin Network, Mobile Seismic Network e SERAPIS Network usate per l'analisi.

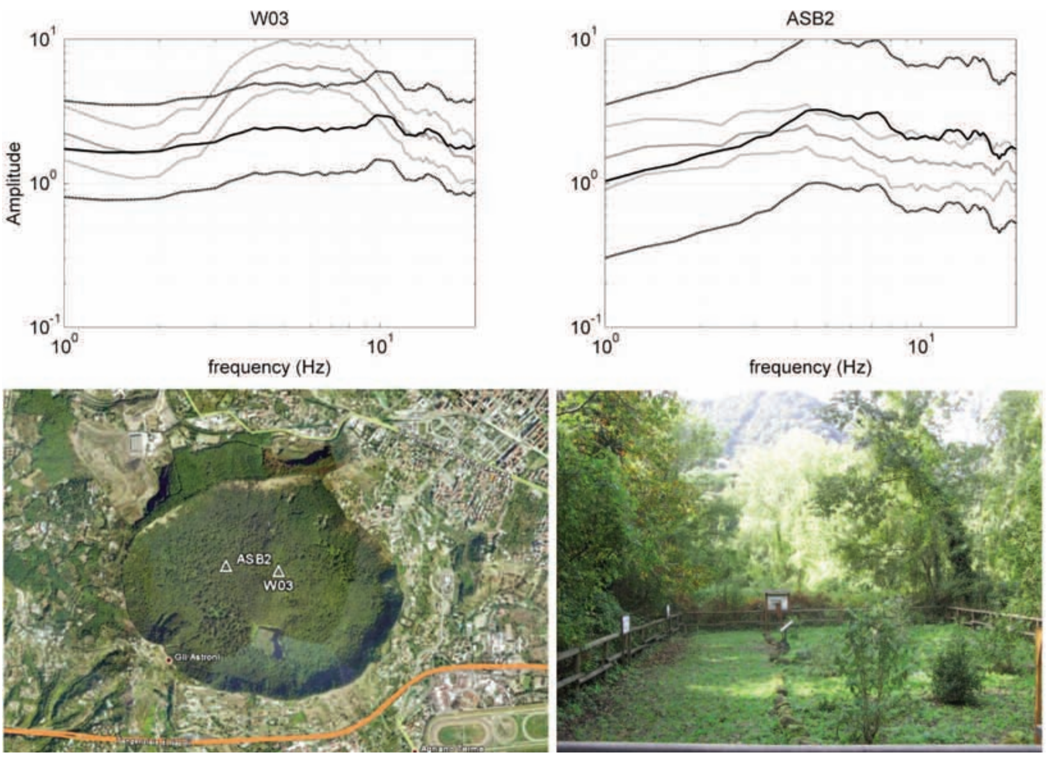

Figure 8 In the top panels we show the site transfer functions obtained with the H/V method (grey) and with the generalized inversion technique (black) for the station W03 (left) and for the station ASB2 (right). The upper and lower lines show the 1 σ error. The bottom panels show the Google Earth image of the stations W03 and ASB2 (left) and a picture of the place where the station ASB2 is deployed (right).
Figura 8 Nei due pannelli superiori sono riportate le funzioni di trasferimento di sito calcolate con il metodo H/V (grigio) e con il metodo delle inversioni generalizzate (nero) per le stazioni W03 (sinistra) e ASB2 (destra). Le curve superiore ed inferiore riportano l'errore: 1 σ. Nei pannelli inferiori sono riportate immagini tratte da Google Earth delle stazioni W03 e ASB2 viste dall'alto (sinistra) e una foto del sito in cui si trova la stazione ASB2 (destra).

The area where station W03 lies is almost flat and belongs to the WWF reserve. The transfer function of this site calculated with the H/V method shows an high peak (amplitude >2) between 3 and 10 Hz, but the same is not verified for the curve calculated using the inversion technique (see the top left panel of Fig. 8). This inconsistency can be related to lateral propagation effects (basin shape), as Bindi et al. [2009] noticed for the Gubbio basin, central Italy. These authors observed that the site located inside the basin are characterized by broad frequency band amplifications and the amplification pattern does not exhibit a strong dependence on the site location as in the case of 1D response.
Station ASB2 is located about 600 m far from W03; the bottom right panel of Fig. 8 shows a picture of the site. The site transfer function of this station calculated with the H/V method shows a low peak for the same frequency band as station W03 (3-10 Hz). The transfer function calculated with the inversion method shows a similar shape but the maximum amplitude is reached in the frequency band 4-7 Hz.
The two sites transfer functions are characterized by broad frequency-band amplification (estimated with the HVSR method), rather than well-defined amplification peaks. This could be explained in terms of low contrast in the stratified medium underlying the station, however the differences found in the W03 site transfer functions calculated with the two methods (HVSR and GIT) are better explained in terms of basin effects, considering also the fact that there are not particular differences in the local geology of the whole basin.

4.2 The Camaldoli hill

Two seismic stations were located on the Camaldoli hill: W05 belonging to the WN and CAM belonging to the SN (see bottom right panel of Fig. 9). Station W05 was located at the top of the hill, inside the gardens of the Camaldoli monastery, close to the border of a high angle scarp. This scarp has been generated during collapse of the two calderas of Campi Flegrei. Station CAM was located more to the North where the slope is more gentle. These sites are very close to each other, and their two STFs calculated with the H/V technique showed a peak at low frequencies. The site transfer function of the CAM station has a peak between 3 Hz and 5 Hz, while the one of the W05 station has a peak for frequencies <4 Hz (see top panels of Fig. 9). For station

W05, the site transfer function calculated with the inversion method shows a peak (up to 3) at low frequencies (2-4 Hz) (see top left panel of Fig. 9). The peak is probably due to the fact that the station was located at the top of a hill bordered by high angle slopes.

The small difference that is present between the two transfer functions (W05 and CAM) is probably due to the difference in the slope of the hill, as suggested by Lee et al. [2009] that used spectral element in Yangminshan Region of Taiwan to show that at mountain top the amplification increases

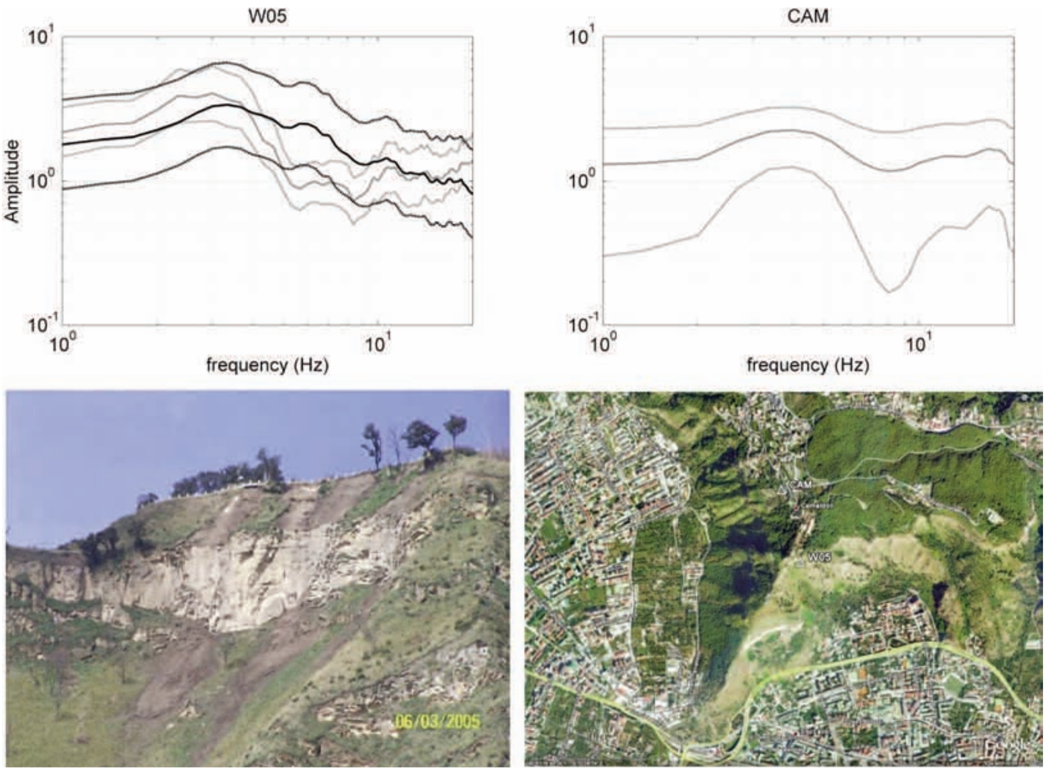

Figure 9 In the top left panel we show the site transfer functions obtained with the H/V method (grey) and with the generalized inversion technique (black) for the station W05. For the station CAM (belonging to the SN) we show the site transfer function obtained with the H/V method (top right). The upper and lower lines show the 1 σ error. The bottom panels show the Google Earth image of the stations W05 and CAM (right) and a picture of the place where the station W05 was deployed (left).
Figura 9 Nel pannello superiore sinistro sono riportate le funzioni di trasferimento di sito calcolate con il metodo H/V (grigio) e con il metodo delle inversioni generalizzate (nero) per la stazione W05. La funzione di trasferimento di sito calcolata col metodo H/V per la stazione CAM (appartenente al SN) è rappresentata nel pannello superiore destro. Le curve superiore ed inferiore riportano l'errore: 1 σ. Nei pannelli inferiori sono riportate un'immagine tratta da Google Earth delle stazioni W05 e CAM viste dall'alto (destra) e una foto del sito in cui si trovava la stazione W05 (sinistra).

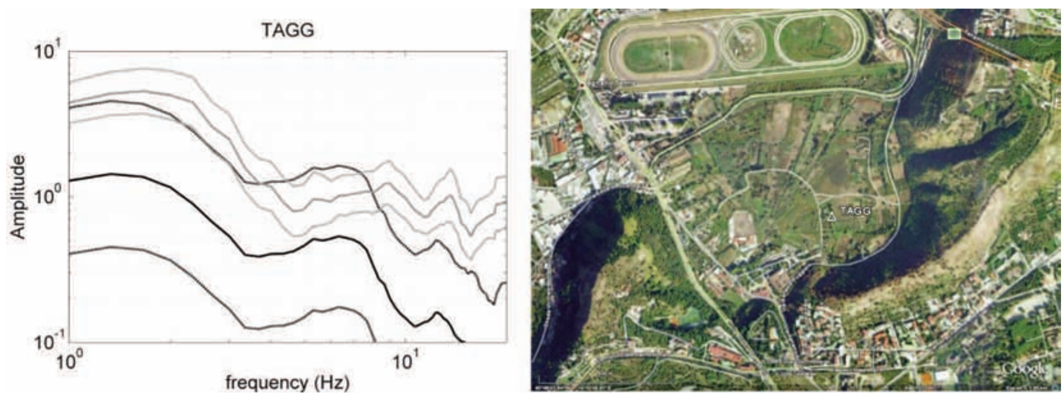

Figure 10 IIn the left panel we show the site transfer functions obtained with the H/V method (grey) and with the generalized inversion technique (black) for the station TAGG. The upper and lower lines show the 1 σ error. The right panel show the Google Earth image of the station TAGG.
Figura 10 Nel pannello di sinistra vengono riportate le funzioni di trasferimento di sito calcolate con il metodo H/V (grigio) e con il metodo delle inversioni generalizzate (nero) per la stazione TAGG. Le curve superiore ed inferiore riportano l'errore: 1 σ. Nel pannello di sinistra è riportata un'immagine tratta da Google Earth della stazione TAGG vista dall'alto.

depending on topography gradient and scale. Nevertheless, there are no particular differences in the geological characteristics of the sites where these two stations were installed. Infact the Camaldoli hill is composed of a thick sequence of zeolitized or welded tuffs (type B deposit) with almost no differences in the velocity parameters. Only the upper part of the sequence is a 30 m thick succession of non-cohesive ash and pumice lapilli layers interbedded to paleosoils (type A deposit). This sequence could influence the site transfer functions but it does not justify the differences between the site transfer functions of the two stations located on the hill.

4.3 The Agnano plain

Inside the Agnano plain, produced by the volcano-tectonic collapse occurred during the Agnano - Monte Spina eruption [de Vita et al., 1999], lies the station TAGG. The location is reported in the right panel of Fig. 10.

The site transfer function calculated with the H/V method shows a very high peak at low frequencies (1-3 Hz) then the function becomes lower than one. The same shape is obtained with the inversion technique, but in this case the function is shifted to the bottom of the plot and the peak reaches the amplitude of 1.5 (see left panel of Fig. 10).

This station has a geologically interesting location as it is placed almost on a wetland. The station lays on the palustrine deposits (type D deposit) of the Agnano lake characterized by very low S-wave velocity and low density ($\rho \simeq 0.9 gr/cm^3$). These deposits cause a high site transfer function at a frequency that depends on the thickness of the layer, which, on the basis of the available boreholes, is about 25m thick and overlay denser ($\rho \simeq 1.5 gr/cm^3$) layers 70 m thick (type A and B deposit).

Conclusions

The results of the preliminary site response analysis in the Campi Flegrei area seem to indicate that topographic features are sometimes relevant in the seismic wave amplification. The heterogeneity of the Campi Flegrei structure makes a detailed study of the site amplification properties necessary. We need to understand when the stratigraphic properties take the advantage on the topographical ones and vice versa. This objective will be achieved by the determination of all the site transfer functions of the site equipped with a seismometer and the integrated analysis of this information with lithological and topographical information. We wish to determine a relation between this characteristics and to elaborate a microzonation map of the entire Campi Flegrei area. The successive analysis will deal with this aim.

Acknowledgements

This work was supported by the Dipartimento di Protezione Civile of Italy (DPC) and Istituto Nazionale di Geofisica e Vulcanologia (INGV) in the framework of the projects entitled "SPeeD". The authors wish to thank Edoardo Del Pezzo, Simona Petrosino, Paola Cusano and Eliana Bellucci Sessa for their useful suggestion and the referee Giuliano Milana which improved the quality of the paper.

References

Andrews, D. J. (1986). *Objective determination of source parameters and similarity of earthquakes of different size in Earthquake Source Mechanics*, American Geophysical Union, Washington.

Aster, R., R. Meyer, G. De Natale, M. Martini, E. Del Pezzo, G. Iannaccone and R. Scarpa (1989). *Seismic investigation of the Campi Flegrei: a synthesis and summary of results*. Editors: K. Aki and P. Gasparini and R. Scarpa. In: Volcanic Seismology, Proc. Volc. series III, Springer-Verlag, San Francisco.

Barberi, F., G. Corrado, F. Innocenti and G. Luongo (1984). Phlegraean Fields 1982–1984: *Brief chronicle of a volcano emergency in a densely populated area*. Bull. Volcanol. 47(2):175–185.

Bindi, D., S. Parolai, F. Cara, G. Di Giulio, G. Ferretti, L. Luzi, G. Monachesi, F. Pacor and A. Rovelli (2009). *Site Amplifications Observed in the Gubbio Basin, Central Italy: Hints for Lateral Propagation Effects*. Bull. Seismol. Soc. Am. 99, 741-760.

Bonilla, L. F., J.H. Steidl, G.T. Lindley, A.G. Tumarkin and R.J. Archuleta (1997). *Site amplification in the San Fernando Valley, California: Variability of site effect estimation using the S-wave, coda and H/V methods*. Bull. Seismol. Soc. Am. 87 (3), 710–730.

Borcherdt, R. D. and J. F. Gibbs (1976). *Effects of local geological conditions in the San Francisco Bay region on ground motions and the intensities of the 1906 earthquake*. Bull. Seismol. Soc. Am. 66, 467–500.

Boatwright, J. and J. B. Fletcher and T. E. Fumal (1991). *General inversion scheme for source, site, and propagation characteristics using multiply recorded sets of moderate-sized earthquakes*. Bull. Seismol. Soc. Am. 81(5), 1754–1762.

Cinque, A. and G. Rolandi and V. Zamparelli (1985). *L'estensione dei depositi marini Olocenici nei Campi Flegrei in relazione alla vulcano-tettonica*. Boll. Soc. Geol. Ital. 104, 327–348.

Del Gaudio, C., I. Aquino, C. Ricco and C. Serio (2009). *Monitoraggio geodetico dell'area vulcanica napoletana: risultati della livellazione geometrica di precisione ese-*

guita ai Campi Flegrei a settembre 2008. Quaderni di Geofisica, 66.

Del Pezzo, E. and G. De Natale and A. Zollo (1984). *Space-time distribution of small earthquakes at Phlegraean Fields*. Bull. Volcanol. 47 (1984), pp. 201–207.

Del Pezzo, E., S. De Martino, M.T. Parrinello and C. Sabbarese (1993). *Seismic site amplification factors in Campi Flegrei, southern Italy*. Phys. Earth. Plan. Int. 78, 105-117.

De Vita, S., G. Orsi, L. Civetta, A. Carandente, M. D'Antonio, A. Deino, T. Di Cesare, M.A. Di Vito, R. V. Fisher, R. Isaia, E. Marotta, M. Ort, L. Pappalardo and J. Southon (1999). *The Agnano–Monte Spina eruption (4.1 ka) in the resurgent, nested Campi Flegrei caldera (Italy)*. J. Volcanol. Geotherm. Res. 91, 269–301.

Di Vito, M., R. Isaia, G. Orsi, J. Southon, S. De Vita, M. D'Antonio, L. Pappalardo and M. Piochi (1999). *Volcanism and deformation since 12.000 years at the Campi Flegrei caldera (Italy)*. J. Volc. Geoth. Res. 91, 221–246.

Drouet, S., A. Souriau and F. Cotton (2005). *Attenuation, seismic moments and site effects for weak motion events: Application to Pyrenees*. Bull. Seism. Soc. Am. 95 (5), 1731-1748.

Field, E. H. and K. H. Jacob, K. H. (1995). *A comparison and test of various siter esponse estimation techniques, including three that are not reference-site dependent*. Bull. Seismol. Soc. Am. 85 (4), 1127–1143.

Galluzzo, D., E. Del Pezzo, M. La Rocca, M. Castellano and F. Bianco (2009). *Site effects at the Vesuvius volcano: a comparison of techniques and inferences as the scaling of law of the seismic spectrum*. Bull. Seismol. Soc. Am. 99 (3), 1705-1719.

Gasparini, P., (1998). *Looking inside Mt. Vesuvius*. EOS Trans., AGU 79, 229–232.

Hartzell, S. H., (1992). *Site response estimation from earthquake data*. Bull. Seism. Soc. Am. 82, 2308–2327.

Judenherc, S. and A. Zollo (2005). *The bay of Naples (Southern Italy): Constraints on the volcanic structures inferred from a dense seismic survey*. J. Geophys. Res. 109, doi:10.129/2003JB002876.

Lachet, C., D. Hatzfeld, P. Bard, N. Theodulidis, C. Papaioannou and A. Savvaidis (1996). *Site effect and microzonation in the city of Thessaloniky (Greece). Comparison of different approaches*. Bull. Seism. Soc. Am. 86 (6), 1692-1703.

Langston C. A. (1979). *Structure under Mount Rainier, Washington, inferred from teleseismic body waves*. J. Geophys. Res. 84, 4749–4762.

Lee, S.-J., Y. C. Chan, D. Komatitsch, B. S. Huang and J. Tromp (2009). *Effects of realistic surface topography on seismic ground motion in the Yangminshan region of Taiwan based upon the spectral-element method and LiDAR DTM*. Bull. Seismol. Soc. Am. 99 (1), 681–693.

Lermo, J., and F.J. Chavez-Garcia (1993). *Site effect evaluation using spectral ratios with only one station*. Bull. Seismol. Soc. Am. 83, 1574–1594.

Lomax, A., J. Virieux, P. Volant and C. Berge (2000). *Probabilistic earthquake location in 3D and layered models: Introduction of a Metropolis-Gibbs method and comparison with linear locations in Advances in Seismic Event Location*. Thurber, C.H., and N. Rabinowitz (eds.). Springer, Kluwer, Amsterdam.

Orsi, G. and S. De Vita and M. Di Vito (1996). *The restless resurgent Campi Flegrei caldera (Italy): constraints on its evolution and configuration*. J. Volcanol. Geoth. Res., 74, 179-214

Nakamura, Y. (1989). *A method for dynamic characteristics estimation of subsurface using microtremor on the ground surface*. Quart. Rep. Railway Tech. Res. Inst. (RTRI) 30, 25–33.

Parascandola, A., (1947). *I fenomeni bradisismici del Serapeo di Pozzuoli*. Genovesi, Napoli.

Parolai, S., D. Bindi and L. Troiani (2001). *Site response for the RSM Seismic Network and Source Parameters in the central Appenines (Italy)*. Pure App. Geophys. 158, 695-715.

Petrosino, S., L. De Siena and E. Del Pezzo (2008). *Re-calibration of the magnitude scales at Campi Flegrei, Italy, on the basis of measured path and site and transfer functions*. Bull. Seismol. Soc. Am. 98 (4), 1964–1974.

Phillips, W. S. and K. Aki (1986). *Site amplification of coda waves from local earthquakes in central California*. Bull. Seism. Soc. Am. 76, 627-648.

Rosi, M. and A. Sbrana (1987). *The Phlegraean Fields*. CNR, Quad. de "La ricerca Scientifica", 114: 1-175.

Santacroce, R., R. Cristofolini, L. La Volpe, G. Orsi and M. Rosi (2003). *Italian active volcanoes*. Episodes, 26 (3): 227-234.

Tsujiura, M. (1978). *Spectral analysis of the coda waves from local earthquakes*. Bull. Earthquake Res. Inst., Tokyo Univ. 53, 1–48.

Wills, C. J., M. Peterson, W. A. Bryant, M. Reichle, G. J. Saucedo, S. Tan, G. Taylor and J. Treiman (2000). *A Site-Conditions Map for {California} Based on Geology and Shear-Wave Velocity*. Bull. Seism. Soc. Am. 90, S187-S208.

Indice

Coordinamento editoriale e impaginazione
Centro Editoriale Nazionale | INGV

Progetto grafico e redazionale
Laboratorio Grafica e Immagini | INGV Roma

Via di Vigna Murata, 605
00143 Roma
Tel. +39 06518601 Fax +39 065041181

http://www.ingv.it

Istituto Nazionale di Geofisica e Vulcanologia